Treatment and visual analysis of numerical simulation of supersonic flows with extensive output after parallel calculation

Boris Rybakin[1], Valery Goryachev[2*]

[1]SRISA, RAS, Moscow State University, Moscow, Russia
[2]Department of Mathematics, Tver State Technical University, Tver, Russia
*corresponding author: valery@tversu.ru

Abstract The present contribution is aimed at numerical modeling and graphic post-processing of data obtained in simulation of three-dimensional hypersonic flow initiated by strong shock wave oncoming on molecular cloud and interaction detailing. Investigations and simulation of supernova explosions and wave processes extended outside by means of cosmic wind have important role in developing of ISM description methods. Numerical solution of task was performed on multicore computers. To increase the prediction quality about billion cell calculation grids were approved. The outlet dataflow after detailed simulation is very extensive. Information treatment for high gradient zones near shock envelopes demand from spectator facility to use the proper visualization tools, first of all an extensive volume or surface rendering, fast tracing of streamlines and surface paths. It is essential to understand the dynamic changeable structure and flow peculiarities to avoid any misunderstanding or artifacts of realignment in stream. Numerical experiments and post-processing were performed using in-house combined GPU and multicore parallelization codes.
Keywords: astrophysical fluid dynamics, shock wave molecular cloud interaction, numerical simulation visualization, gas-dynamical instability

1 Introduction

Strong hypersonic shock wave interaction of compressed ambient gas flow with molecular cloud situated in interstellar medium (ISM) is one of actively investigated task of modeling in astrophysics now. Explosion and propagation of supernova remnants are accompanied by the generation of strong shock wave. Interaction between supernova shock wave and molecular clouds can initiate a radical gas density and dust redistribution in cloud. Fragmentation of MC initiates heterogeneity rise of gravitational field and leads to forming of star systems. Modern astrophysics fluid dynamics codes contain possibility to predict generation of stellar and planetary magnetic fields, to calculate convection and mixing processes in stellar interiors and many others. Originating computer systems comprise fluid dynamics solvers with different level of description. A basis of recent codes was put in the works [1, 2]. The strong shock wave and ambient ISM gas interactions with molecular cloud study mostly in two-dimensional introduction [3, 4]. Advanced three-dimension simulation grows accordingly expansion of processor parallelism on supercomputers. New programs allow settle MC tasks with high accuracy taking into account rising disturbing parameters set, for example to consider perturbations of intermittent layers in interacted phase, that lead to formation of different structures in molecular clouds. Nascent hydrodynamic instabilities generate a gaseous fragmentation, spurs, turbulent flows, and anticipate a start of new stars.
Numerical simulations have become a novel approach in studying such complex flows. Complexity of the problem requires significant computational efforts. One of the first uniform resolution simulations of shock-bubble interaction (SBI) derived from of astrophysics task, have been performed in [5]. Representative results of SBI prediction were presented in work [6]. In paper [7] authors presented the first three-dimensional simulation. Authors of [8, 9] accomplish high detailed 3D simulation and present impressive high resolution visualization of the interactions of a normal shock wave at Mach 3, with a spherical helium bubble immersed in more heavy gas. The governing Euler equations for two-phase compressible flows were solved using a finite volume solver with uniform resolution using billions cells in calculation domain. Code developers employ the 5th order WENO reconstruction of the primitive quantities and the 3rd order TVD Runge-Kutta time stepping scheme. DNS of compressible, two-phase flow was developed to solve above mentioned task in [10]. Adaptive Mesh Refinement approach to increase prediction quality on shock wave interface in high gradients zones of flow was used. Detailed simulations reveal that the shock passage compresses the bubble and generates vorticity on the density interface. Vorticity evolution and compression

in time lead to the formation of a mixed jet, rolled rings and a long lasting vortex core. Two principle cases of fluid prediction for SBI were considered in [11]. The first was the rarefied bubble and the second was the dense bubble which corresponds to quasi-stationary regime with the emergence of stable vortex rings and regime, in which unstable vortex structures appear. Above mentioned numerical experience can be used to get more circumstantial study of shock wave and cloud (bubble) interaction, among them results from works [12, 13] too.

2 Problem definition

Numerical study of compression mechanism, cloud density field fragmentation and whirling flow formation, has been the objective of present contribution.

Developed computational code is based on numerical solution of the Euler equations for compressible flow. Gas flow equations were represented conservatively for velocities components, energy, and pressure.

Statement of problem: the compressed gas with plane frontal shock wave with hypersonic velocity runs into spherical cloud, after initial contact the post-shock interstellar gas interacts with more dense gas of the cloud. The computational area is a parallelepiped with grid dimensions $n_x*n_y*n_z$. On the left and right domain boundaries prescribed the conditions at the open boundary. The remaining boundaries adopted periodic conditions. The time step is found from Courant-Friedrich's-Levy condition of stability. For carrying out systematic calculations mesh sizes of 1024*512*512 were used. The radius of the spherical cloud has a size of 64 cells.

The shock wave, adjacent to the left cloud boundary and at time t=0 begins to interact with the surface border of the cloud. Several of assumptions about model parameters were accepted. Single-phase model for oncoming gas and gas inside of molecular cloud can be used for sufficiently accurate physical process description. Unperturbed interstellar medium consist of relatively heated matter (~10000 K) and cold heterogeneous dispersed molecular clouds (~100 K) that having larger density.

We consider the dynamics of the spherical and (in transition) quasi-spherical clouds after the interaction with shock wave. Initially the cloud is in dynamic equilibrium with the background gas. In our model, we specify the ambient temperature of the interstellar medium $T_a= 10^4$ K, the density $\rho_a=2.15*10^{-25}$; in the cloud at undisturbed state $T_c=100$ K, $\rho_c=1.075*10^{-22}$. We represent cloud as spherical surface of the radius $r_c=0.05$ pc. In the calculations we neglect gravity, the effects of the heat conduction and radiation losses taking the ideal gas state equation with a factor of an adiabatic $\gamma = 5/3$. The gas parameters behind the shock wave are determined from Rankine-Hugoniot equation. The Mach number of the shock wave is equal to M=7, density $\rho_{sh}=8.6*10^{-22}$ g/sm^3, temperature $T_{sh}=1.5*10^5$ K, speed of shock wave $u_{sh}= 104$ km/s. The thickness of the shock wave front is large enough ~ 2-5 pc, which is much greater than the radius of the cloud. The cloud radius is $r_c=0.05$ pc, the time of passage of the shock wave over clouds is equal to 960 years. In calculations dimensionless quantities were carried out. Cited below results are given in dimensionless form. We neglect in simulation any radiation losses, heat conduction, and gravitational forces. Possible model complications can be scheduling in the next simulation enhancement.

3 Numerical realization

High-resolution schemes were tested; one of them was TVD modification [14]. Such second order accurate non-linear scheme with limited overall variation enable to calculate shock waves with high resolution and prevent non-physical oscillation on their fronts. Among these schemes, preference is given to schemes that allow parallel realization algorithms, which enable calculations on heterogeneous computing systems using graphic accelerators. Program versions were written for these schemes, and 3D tests were conducted [12, 13]. Good coincidence of predicted, analytical and experimental data has been achieved using meshes from 128^3 до 1024^3. Front of shock waves is spread out over 3-5 calculation cells. Parallel algorithms using OpenMP technology for several cores of processors and graphic accelerators from NVIDIA (using CUDA) were developed. To enhance code efficaciousness it is necessary to use large-scale main storage and to conduct memory allocation between CPU and GPU, to reduce interchange processes. Tasks with large amount of data were performed using control of redistribution of real RAM on computers with GPU. For the task under discussion usable in-house code permitted to accelerate calculations more than seventeen times is used.

To do a quality analysis of complicated space-time scenes of structure formations under review we have used a different approach and tools to visualize flow simulated. Processing of extensive output data, visualization of unsteady flow fields and identification of vortex structures were performed using in-house system HDVIS. Among enhanced post-processing function it has an embedded calculator for on-demand computation of a large set of useful gas dynamic quantities, their combinations and spatial derivatives. This feature facilitates the analysis of the numerical results. Detailed explanations of simulated flows with strong gradient zones was done taking into account the high resolution behavior of flow closely to clustered distensible (contractible) shock wave envelopes, origin and break-up of inner waves, curling and twisting of vortex break-up and other effects. Visualization and animation of instantaneous scalar and vector fields were performed using derived variable fields. These additions were used in linked combinations for representing of results more substantial.

4 Consideration and analysis of numerical solution

Visualization and treatment of numerical solution results of simulated interstellar shock cloud interaction (SCI) are presented below. Illustrations are presented by figures 1-5.
During of interaction several specific stages of SCI are elapsed. The time frames of interaction process are illustrated using density gradient contours (shlieriens) on figure 1. The first fragment (1) corresponds to cloud and shock wave front positions at time t=1, first go after initialization of shock interaction. Inside adiabatically balanced gas dense matter of cloud forward and reflected wave begin to spread. Inner-cloud gas behind wave front begins to contract. Velocity of density perturbation inside cloud sub-layer is less more than an order of one in ISM and more less of main shock wave velocity. Bow wave skirts around the cloud at time t=22. By this time a reverberated from cloud reflexive wave begins to move toward the post-shock flow. Due to it, local perturbation of density start to develop, that is shown for frame time more sixteen. More dense and heavy gas begins to move left from initial cloud center and starts to deform a left boundary surface layer. This wave over interaction with oncoming frontal post-shock wind can spread with minor velocity, than inner wave inside cloud. It can reinforce the wave expansion damping.
On the right cloud boundary Richtmyer-Meshkov (RM) instability stems from provoked by shock wave a deviation from original intention of the density distinguish in boundary sub-layers to decrease inner energy interface. These perturbations are good observable at time more thirty on frames of figures 1 and 3. After transmission of a shock wave via space distance of one initial diameter of spherical cloud the profile of forward shock wave becomes concave. Owing to inner wave reflection ternary Mach legs are forming. Behind shock wave front a primary vortex can form (it leaves a calculation domain after time t=63). Post-shock stream interacts with cloud surface, amplify a perturbation waves on it.
During undulating interaction the process of fragmentation and ablation of cloud sub-surface gas matter become to increase, periodically abating. On figures 2, 3, 4 perturbed pitted and crumpled surface dense layers are shown, post-processing of which can be used for comprehension of dynamic conversations in cloud matter. The ablation and fragmentation processes are going in recirculating zones in leeward side more intensively. At a late phase of SCI intensification of fragmentation and certain structural readjustment of cloud coherent structures are observed. Among them the filamentary structure, shown on figure 4, had found out.
One of the phases of density redistribution is shown on figure 2. The part of path lines start from oncoming gas outside. Other path lines have origin focused in the center of cloud initial position. Heavy gas inside the cloud can dilate with displacement of the origin center to the left. Gas flow can change direction of the moving at different stages. Path lines are turn, twist, expand, and contract in recirculation zone behind of disturbed interphase of cloud layers.
The cloud fragmentation is initiating from hind zone of cloud by reverse reflected shock wave. It is shown on figure 1 with depicted gradient of density function distribution for time position more t=20, after shock wave could pass one cloud diameter. First go as shock wave begins to interact with cloud matter the RM-instability process switches on. Perturbation leads to vorticity generation over surface density layers. Curved shock wave envelope the cloud generates in the immediate vicinity of cloud (in conventional surface) vortex rings of changeable diameter in main and azimuth direction.

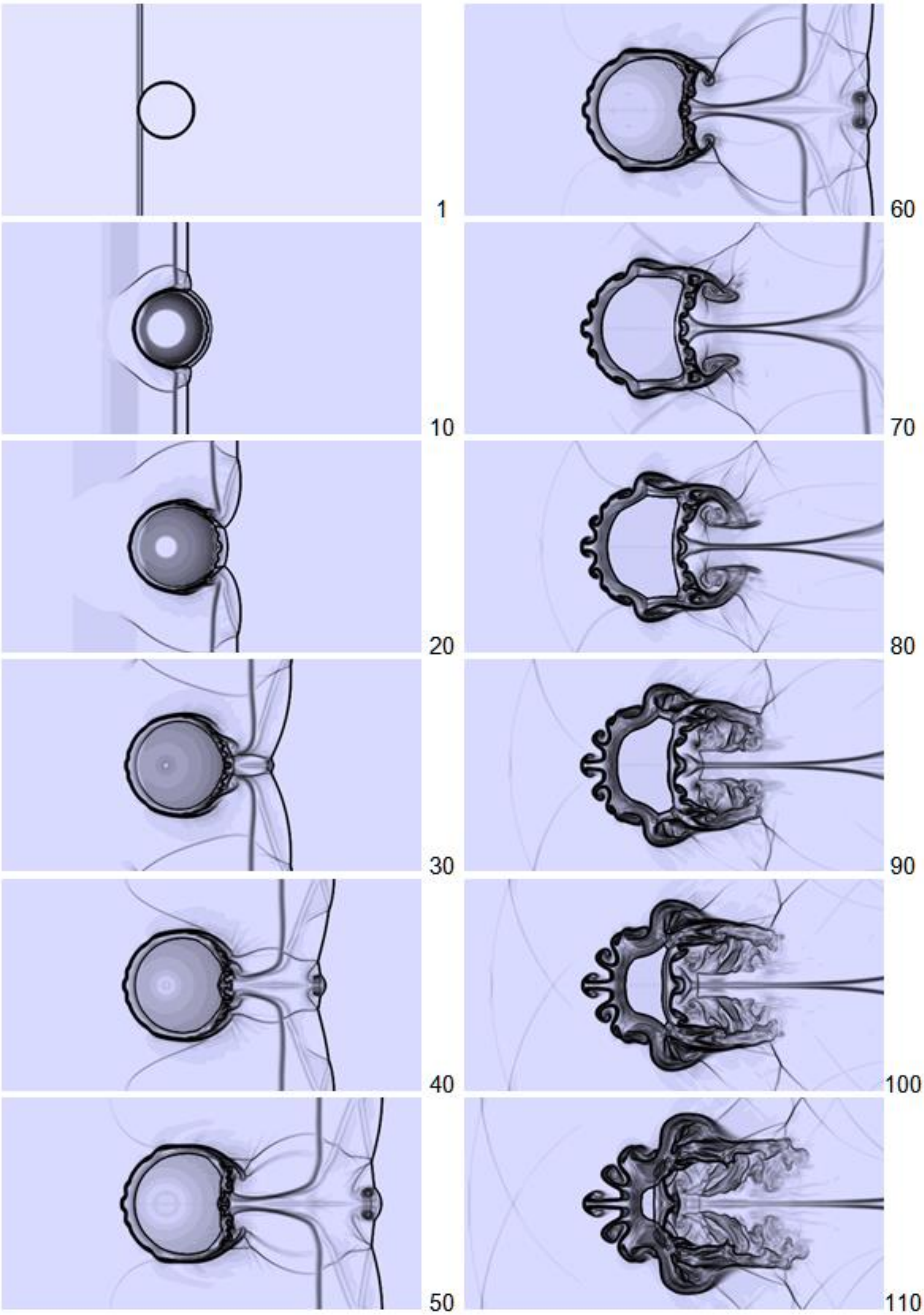

Fig. 1 Frames of numerical schlierens - $|\boldsymbol{grad}(\rho)|$ of ISC interaction

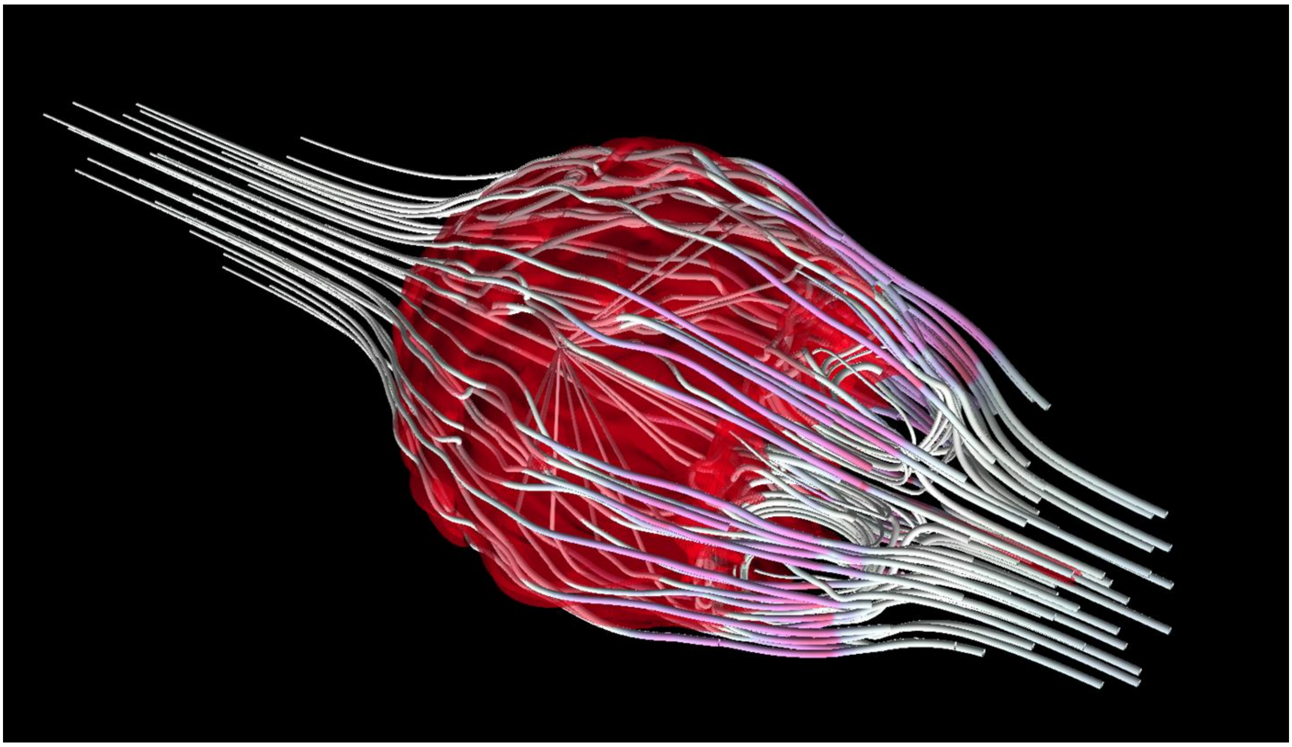

Fig. 2 Path lines and iso-surface of inter cloud logarithmic density log(ρ)=1 at t=70

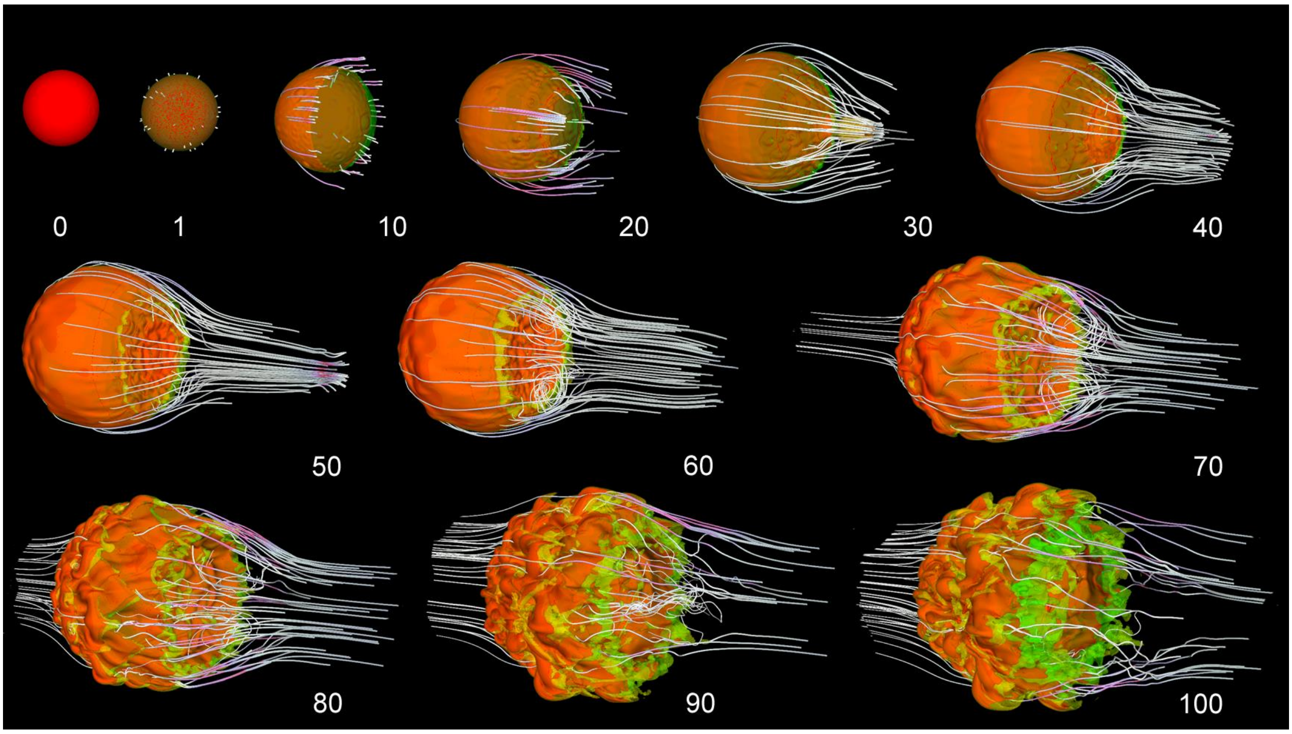

Fig. 3 Time history of cloud superficial layers perturbation, demonstrated in presentation of rendering iso-surfaces for logarithmic density log(ρ)=3 (red solid) and log(ρ)=2 (clear green glow)

Shock interaction stimulates cloud molecular gas to be ablated by the post-shock flow. This process illustrates by state of density and translucent vortex-derivative artificial fields on figure 4 and 5. At time 90 the RM-instability reduces to volume density fragmentation with fuzzy interface. Iso-surface of density (ρ=3) on figure 4 are covered by vortex multi-layer envelopes to amplify imagination about visualized gas formations.

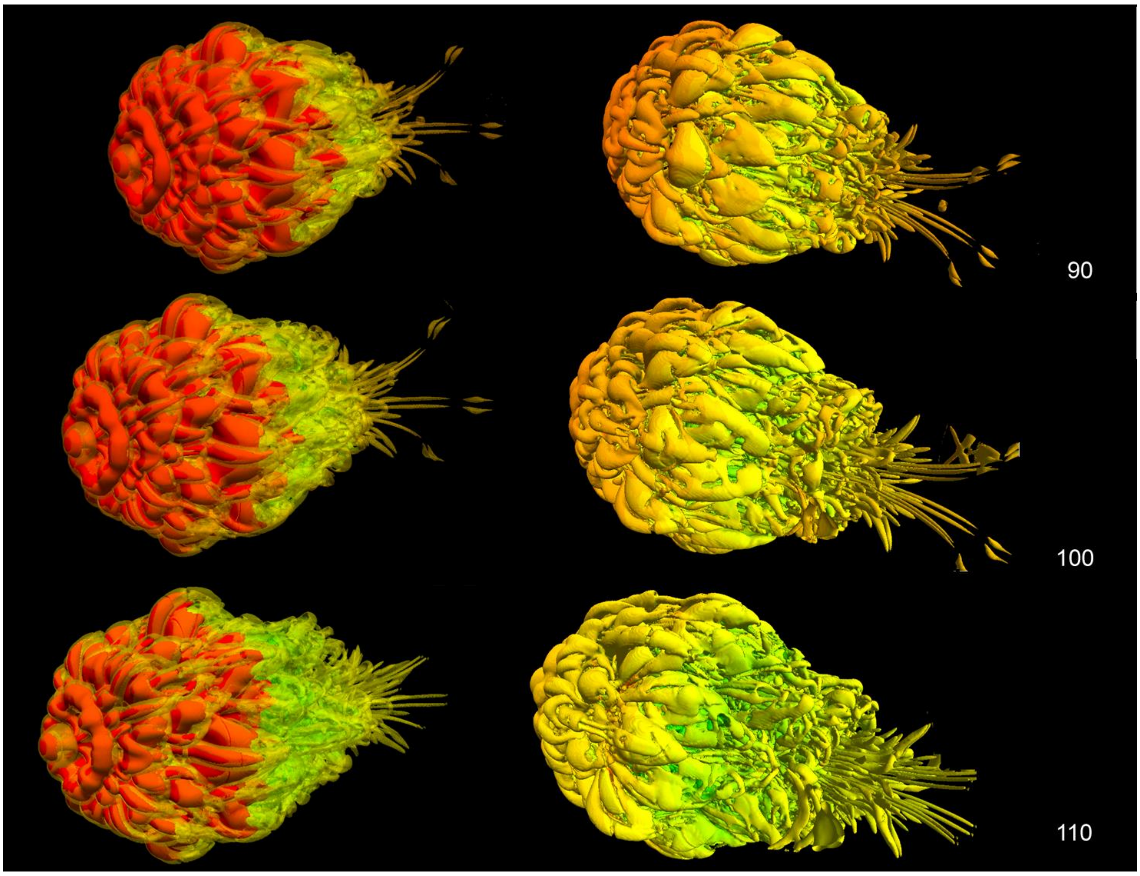

Fig. 4 Fragmentation of shocked cloud, density (red) and superficial layers perturbation, shown by Q-criterion

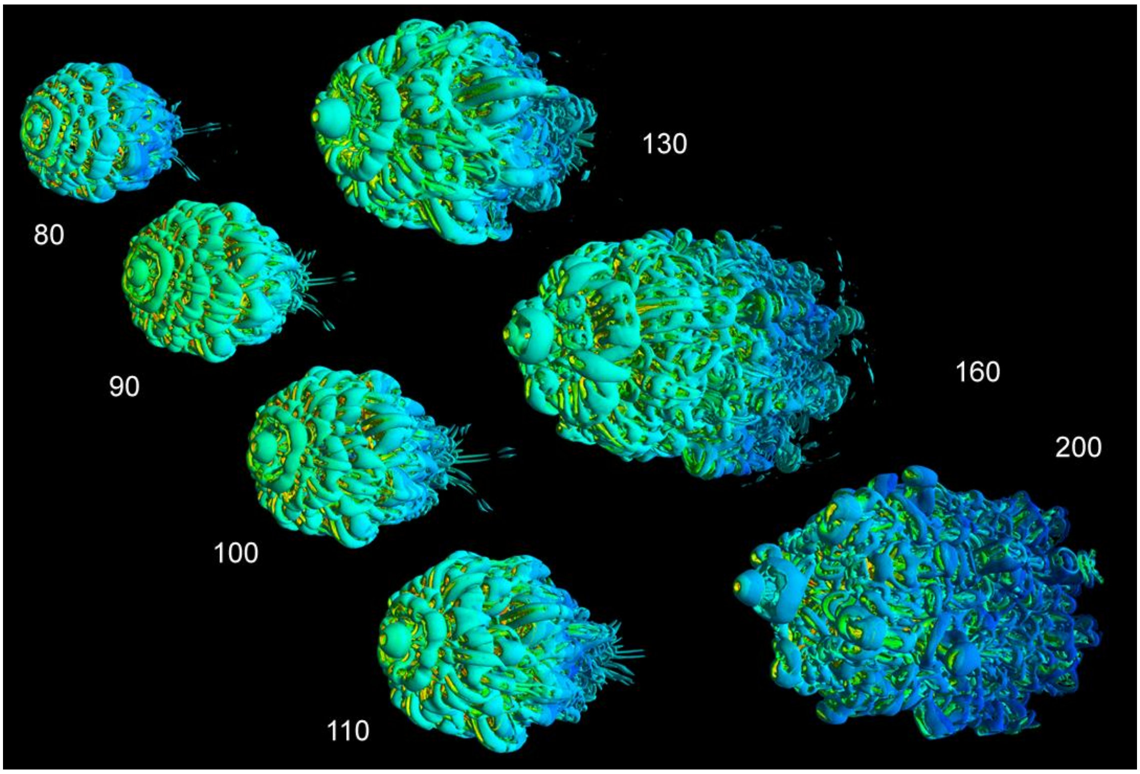

Fig. 5 Time evolution of Q-criterion fields for molecular cloud, iso-surfaces Q=10

The coherent vortex structures of the flow with formation of ring-shaped and directed stream wise finger-like packing, elapsing by hairpin vortices of different scale, are observed. They are visualized using field rendering of the second invariant of the velocity gradient tensor - Q-criterion [15].
Incipient vortices arise in transversal rolls-rings structures over the cloud surface at the start of post-shock wind and cloud interplay. First rolls are converted to elongated vortex legs and initiate a vortex hairpin or plumed structures. Neighbor counter-rotating primary and secondary vortices turns on a new tract level. Visual evidence of local swirl discharge from within surface gas layer is shown on figure 5 (fragment for t=130). Conditional vortex jet “burst open”. This vortex formation cover core vortex line extracted. According to time developing such formations can stretch or bend and can change its shape to hairpin-like form. Time conformity leads to repetition of secondary, tertiary and so on hairpin branch formations. This can be shown on time fragmenting continuation of the Q-criterion fields on figure 5 for t=160 and t=200. The color palette (from turquois to deep-blue) used for iso-surfaces fits the cloud density value from 2 to 0.2. Clear carmine color on shadowy inner side of Q iso-surface fits the density in place with value more than one (initial core thickness). Visual analysis shows how during interaction ring-shaped sinuosity rolls pass throw expanded fragmenting cloud. Observed coherent structures: hairpins (or horseshoe vortices), arched, rolls, plumes and filamentary structures become more small and more tangled, according as time evolution, but repeat primary forms as fractal objects.

5 Conclusions

Numerical modeling of interaction between ISM shock wave from supernova and molecular cloud was performed. The Mach number falling in a strong shock wave was equal to 7. The difference in density between cloud matter and interstellar gas was accepted equal 500. For thorough investigation of arising flow calculation grid with dimension1024×512×512 was used. Treatment of results shows how the fragmentation and collapse of cloud could be occur in adjusted situation using only adiabatic gas dynamics behavior. Combined methods of post-processing allows to find out some of the details of perturbed mass transfer in surface layers of cloud and its influence on ablation and erosion phenomena.

Acknowledgments

The work was supported by the Russian Foundation for Basic Research under grant contracts No.14-07-00065, 14-29-06055.

References

[1] Klein R, McKee C, and Colella P (1994), On the hydrodynamics interaction of shock waves with interstellar clouds, 1. Nonradiative shocks in small clouds. *ApJ*, vol. 420, pp 213-236.

[2] McKee C (1988), Supernova remnant shocks in an inhomogeneous interstellar medium. In Supernova Remnants and the Interstellar Medium, IAU Coll. 101, eds. R. S. Roger & T.L. Landecker, Cambridge University Press, pp 205-222.

[3] Melioli C, de Gouveia Dal Pino E, and Raga A (2005) Multidimensional hydro dynamical simulations of radiative cooling SNRs-clouds interactions: an application to starburst environments. *Astronomy & Astrophysics*, vol. 443, pp 495-508.

[4] Frank A, Poludnenko A, Gardiner T, Lebedev V, Drake R (2003), Stellar outflows with new tools: advanced simulations and laboratory experiments. *RevMexAA (Serie de Conferencias),* 15, pp 85-91.

[5] Quirk J, Karni S (1996) On the dynamics of a shock-bubble interaction. *J. Fluid Mech.*, vol. 318, pp 129–163.

[6] Johnsen E and Colonius T (2009) Modeling of III-D Numerical Simulation of Non-spherical Bubble Collapse. *J. Fluid Mech.*, vol. 829, pp 231–262, Cambridge University Press, doi: 10.1017/S0022112009006351.

[7] Stone J M and Norman M L (1992) The three-dimensional interaction of a supernova remnant with an interstellar cloud, *APJL*, vol. 390, pp 17–19.

[8] Hejazialhosseini B, Rossinelli D, Koumoutsakos P (2013) Vortex dynamics in 3D shock-bubble interaction. *Physics of Fluids*, 25, 110816 (2013), http://dx.doi.org/10.1063/1.4819345.

[9] Hejazialhosseini B, Conti C, Rossinelli D, Koumoutsakos P (2013) High performance CPU kernels for multiphase compressible flows. In: Lecture Notes in Computer Science, 7851, Springer, Berlin, pp 216-225.

[10] Hejazialhosseini B, Rossinelli D, Conti C and Koumoutsakos P (2012) High throughput software for direct numerical simulations of compressible two-phase flows. In: Proceeding of Int. Conf. for High Performance Computing, Networking, Storage and Analysis, Salt Lake City, USA, pp 1-12.

[11] Korneev B. A., Levchenko V. D. (2014) Effective numerical simulation of the gas bubble-shock interaction problem using the RKDG numerical method and the DiamondTorre algorithm of the implementationflows. *Keldysh Institute preprints*, 2014, № 097, Moscow, Russia. 12 p.

[12] Rybakin B (2013) Modeling of III-D Problems of Gas Dynamics on Multiprocessing Computers and GPU. *Computers and Fluids*, vol. 80, pp 403–407, doi: 10.1016/j.compfluid.2012. 01.016, 31-Jan-2012.

[13] Rybakin B, Goryachev V (2014) The supersonic shock wave interaction with low-density gas bubble. *Acta Astronautica*, Vol. 94, Issue 2, pp 749–753.

[14] Jiang G, Tadmor E (1998) Nonoscillatory central schemes for multidimensional hyperbolic conservation laws. *SIAM J Sci Comput*, vol. 19 (6), pp 1982–1917.

[15] Hunt J, Wray A and Moin P (1988) Eddies, streams, and convergence zones in turbulent flows, Proc. Summer Program Center for Turbulence Research (NASA Ames/Stanford Univ.), pp 193-208.